Environmental Modeling & Assessment
https://doi.org/10.1007/s10666-024-09972-y

RESEARCH

Can Turbidity Data from Remote Sensing Explain Modelled Spatial and Temporal Sediment Loading Patterns? An Application in the Lake Tana Basin

Albert Nkwasa[1,2] · Rediet Esayas Getachew[1] · Katoria Lekarkar[1] · Estifanos Addisu Yimer[1] · Analy Baltodano Martínez[1] · Ting Tang[2,3] · Ann van Griensven[1,4]

Received: 9 August 2023 / Accepted: 11 March 2024

Abstract
Understanding the spatial and temporal patterns of sediment loading in water bodies is crucial for effective water quality management. Remote sensing (RS) has emerged as a valuable and reliable tool for monitoring turbidity, which can provide insights into sediment dynamics in water bodies. In this study, we investigate the potential of turbidity data derived from RS to explain simulated spatial and temporal sediment loading patterns in the Lake Tana basin, Ethiopia. Utilizing existing RS lake turbidity data from Copernicus Global Land Service (CGLS) and simulated seasonal and multiyear trends of river sediment loadings into Lake Tana from the Soil and Water Assessment Tool (SWAT + model), we estimate correlations at different river inlets into Lake Tana. The results reveal a strong positive correlation ($R^2 > 0.66$) between the multiyear monthly average sediment load from inflow rivers and RS lake turbidity at most river inlets. This indicates that the simulated river sediment loads and lake turbidity at river inlets exhibit similar seasonal patterns. Notably, higher turbidity levels are observed at the river inlet with the highest sediment load export. These findings highlight the potential of RS turbidity products in characterizing temporal and spatial patterns of sediment loadings, particularly in data-scarce regions, contributing to a better understanding of water quality dynamics in such areas.

Keywords Sediment loading · Turbidity · Remote sensing (RS) · SWAT + · Lake Tana

1 Introduction

In recent years, the Ethiopian highlands have experienced an accelerated rate of soil erosion due to factors such as long-term intensification of land use, climate change, erosion-prone topography, and limited interventions [1, 2]. Soil erosion and sediment redistribution in the highlands have thus gradually evolved to become a critical environmental problem that undermines agricultural productivity, economic sustainability, and the quality of water resources within these areas [3]. Abebe and Minale [4] highlighted a significant transformation in the Lake Tana basin's land use and management since the 1980s. Between 1986 and 2013, the expanse of cultivated land doubled. This change intensified the basin's vulnerability to soil erosion [5]. Notably, an estimated 18.4% of the basin is now considered highly susceptible to erosion with an average sediment yield fluctuating between 30 and 155 ton ha^{-1} yr^{-1} [6, 7]. The accompanying sediment deposition from soil erosion into Lake Tana has consequently led to an increase in lake turbidity and overall decline in lake productivity [8, 9]. The rise in sediment and nutrient inflow into the lake has also been linked to the incidental occurrence and spread of water hyacinths since 2011 [10]. Considering the economic and livelihood significance of the lake to the surrounding

✉ Albert Nkwasa
albert.nkwasa@vub.be

1 Department of Water and Climate, Vrije Universiteit Brussel (VUB), 1050 Brussels, Belgium

2 Water Security Research Group, Biodiversity and Natural Resources Program, International Institute for Applied Systems Analysis (IIASA), Schlossplatz 1, A-2361, Laxenburg, Austria

3 Climate and Livability Initiative, Center for Desert Agriculture, King Abdullah University of Science and Technology, Thuwal, Saudi Arabia

4 Water Science & Engineering Department IHE Delft Institute for Water Education, 2611 AX Delft, the Netherlands

Published online: 25 March 2024

inhabitants, the importance of safeguarding the lake water quality cannot be over emphasized. This necessitates the analysis of the processes within the catchment that contribute to soil erosion and sediment loading into the lake.

Several studies have employed process-based models like the Soil and Water Assessment Tool (SWAT [11] and SWAT + [12]) to investigate the response of sediment loads to changes in climate, land-use, and land management practices within the basin [13–15]. These studies have greatly contributed to the understanding of sediment processes within the basin but have been limited by the inadequacy of in situ sediment load data, which is required for validating the performance of sediment modelling processes. The lack of extensive water quality data, particularly long-term records, is a significant challenge and impedes effective water quality assessment and management in several global regions, such as Africa and Southeast Asia [16]. Recognizing this scarcity of sediment load data in the Lake Tana basin, researchers have sought alternative methodologies. For example, Lemma et al. [2] and Yasir et al. [17] developed empirical relationships, such as rating curves, between discharge and sediment concentration to estimate sediment load in the basin. However, these rating curves are influenced by seasonality, which affects their reliability [6]. Moreover, sediment concentrations in these studies are derived from a limited number of costly and labor-intensive field campaigns, resulting in spatial and temporal coverage limitations. Consequently, the statistical predictive power of these empirical relationships may be insufficient when considering long-term and seasonal sediment load patterns.

To overcome these limitations, remotely sensed water quality datasets have emerged as a valuable and cost-effective compliment to in situ measurements, offering consistent broader spatial and temporal coverage. Remote sensing (RS) has been employed for over 40 years to monitor inland water bodies, especially in areas with limited in situ data [18–20]. RS provides consistent temporal data and has been used to study the spatial–temporal variation of optical water quality parameters such as trophic state and turbidity [21, 22]. Of specific interest in this study is the RS turbidity of inland waters which is fundamental as it is closely linked to sediment fluxes in rivers and lakes. Monitoring turbidity aids in assessing sediment discharge, seasonal variability, and long-term evolution of sediment budgets within catchments [23].

In the Lake Tana basin, previous studies have explored the link between satellite-based imaging, turbidity, and suspended sediment concentration [24, 25]. They have demonstrated the potential of RS measurements to establish long-term water quality databases, which serve as a baseline for trend studies and water resource management, especially in data-scarce regions like the Lake Tana basin. However, there is a scarcity of research on the utilization of RS water quality data to inform water quality models, specifically regarding the comparison of RS water quality products and simulated water quality variables [25]. Notably, there is a gap in research regarding the use of RS turbidity to explain the spatial and temporal variability of simulated river sediment loads by water quality models, despite the strong correlation between turbidity and sediment load. Nonetheless, RS water quality products present a unique opportunity to overcome the limitations of in situ data concerning assessing the spatial and temporal variability of sediment loading [23].

This study aims at assessing the feasibility of utilizing existing RS lake turbidity data to explain both the spatial patterns and the seasonal and multiyear temporal patterns of modelled river sediment simulations within the Lake Tana basin. To achieve this, we employ the SWAT + model [12], which has demonstrated successful application in sediment modelling at large scales [1] and utilize the RS lake turbidity from the freely available products by the Copernicus Global Land Service (CGLS, https://land.copernicus.eu/global/). By establishing correlations between modelled river sediment loads and RS lake turbidity data, we aim to bridge the gap between RS water quality data and water quality modelling, contributing to a more comprehensive understanding of water quality dynamics in data-scarce regions like the Lake Tana basin. The findings of this study have implications for improving the evaluation of sediment modelling and supporting effective decision-making in managing sediment-related issues in freshwater systems.

2 Materials and Methods

2.1 Study Area

The Lake Tana basin (Fig. 1) is situated in northwestern Ethiopia, geographically spanning between 10.95–12.78° N latitude and 36.98–38.25° E longitude [26]. With a total drainage area of 15,096 km^2, the basin comprises Lake Tana, which covers 20% of the area and serves as the source of the Blue Nile (Abay) [27]. Lake Tana, the largest lake in Ethiopia, spans 3111 km^2 and reaches a maximum depth of 15 m, situated at an elevation of 1800 m [27]. The lake holds significant importance for large-scale irrigation, hydropower generation, commercial fishery, agricultural production, and ecotourism and supports various endemic bird species [28]. Moreover, Lake Tana serves as a major water supply for parts of Bahir Dar city, located on its southern shore, as well as neighboring rural regions [8].

The basin experiences a tropical highland monsoon climate, with the primary rainy season occurring from June to September [6]. The mean annual rainfall in the catchment ranges from 805 to 2395 mm, while the mean annual

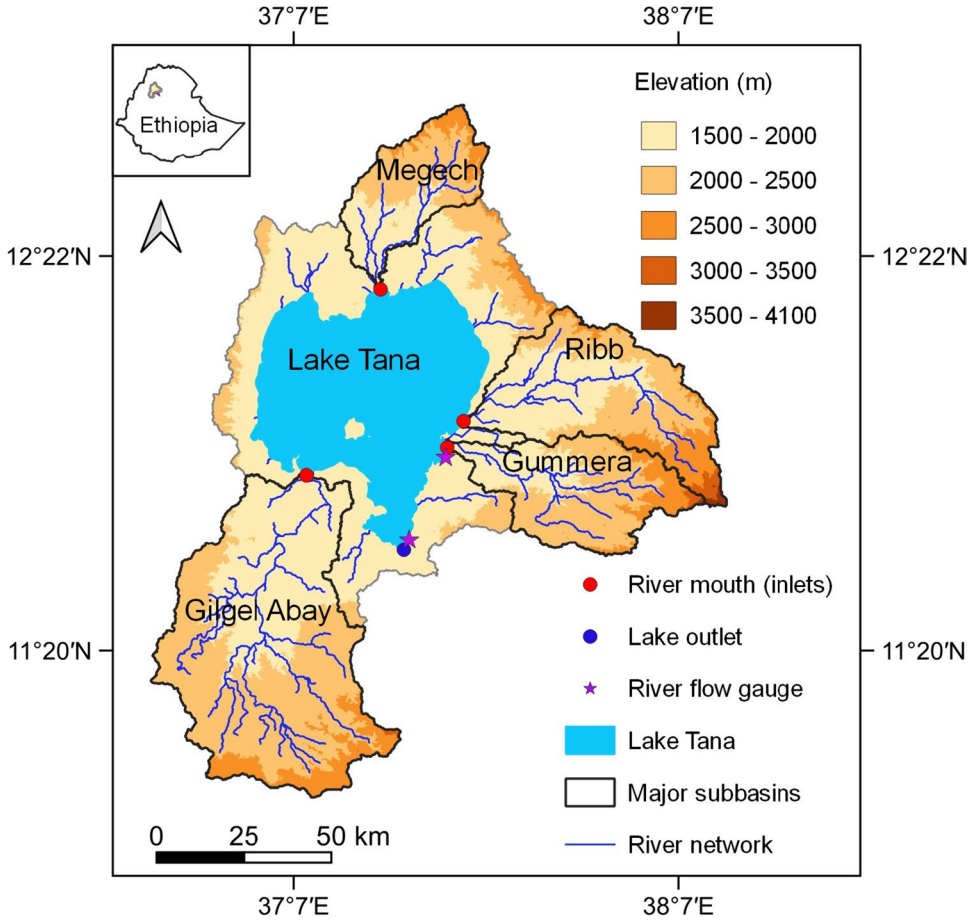

Fig. 1 Study area—Lake Tana basin and the four major sub-basins

evapotranspiration (ET) is approximately 773 mm [27, 28]. Air temperature displays diurnal fluctuations, with daily temperatures ranging between 9 and 28 °C and averaging around 20 °C [27].

Within the Lake Tana basin, the four major subbasins, namely Gilgel Abay, Gummera, Megech, and Ribb (Fig. 1), are undergoing land use and land cover changes, contributing to more than 50% of the incoming sediment load to the lake [9]. These changes involve the conversion of natural vegetation areas especially forested areas to cropland and pasture [29]. Specifically, there has been a 31% expansion of agricultural land and a 16% increase in built-up areas over the past 30 years (from 1989 to 2019) across the entire basin [30]. At the subbasin level, in the Gilgel Abay subbasin, cultivated land cover significantly increased from 26.1% in 1973 to 41.2% in 2008 [6]. Agricultural land use in the Gummera subbasin doubled in 40 years between 1973 and 2013 [31]. As of 2018, 88% of the Ribb subbasin was covered by agricultural land [32], while in the Megech subbasin, forests account for only 3% of the land, and 47% of the watershed area is classified as prone to erosion [33]. The steep slope in the Megech subbasin exacerbates erosion processes. Soil erosion represents a significant watershed issue in the Lake Tana basin, resulting in substantial loss of soil fertility, reduced productivity, and increased lake turbidity [34].

2.2 Model Description

SWAT + is a river basin scale, physically based and semi-distributed model developed to simulate the long-term impacts of land management practices on water, sediment, and nutrients in watersheds [12]. It is an improved version of SWAT that has been revised to allow for greater flexibility in delineating and configuring watersheds. Although the basic computational algorithms are retained, landscape units (LSUs) are introduced to improve the representation of subbasin land areas. SWAT + can also be used to define management schedules and connect natural flow streams to managed flow systems using decision tables [35, 36]. LSUs store topographical data that is useful to calculate concentration time and are further subdivided into hydrologic response units (HRUs). HRUs describe the area's spatial heterogeneity in terms of the unique combination of land use, soil type, and slope [12]. They are the primary calculation units for simulating all hydrologic processes, and the results are aggregated at the subbasin level [11].

The model uses water balance equation given by Neitsch et al. [37] (Eq. 1), to accurately simulate the hydrological processes within the basin before it can realistically predict the sediment yield [38].

$$\mathrm{YB_f} = \mathrm{YB_i} + \sum_{j=1}^{t}(P_j - R_j - E_j - D_j - \mathrm{RF_j}) \quad (1)$$

where $\mathrm{YB_f}$ is the final soil water content, $\mathrm{YB_i}$ is the initial soil water content (mm) on day j, t is the time (days), P_j is the amount of rainfall (mm) on day j, R_j is the amount of surface runoff (mm) on day j, E_j is the evapotranspiration amount (mm) on day j, D_j is the percolation amount (mm) on day j, and $\mathrm{RF_j}$ is the return flow amount (mm) on day j.

The Modified Universal Soil Loss Equation (MUSLE) is used to calculate soil erosion at the HRU level (Eq. 2). The soil erosion prediction is dependent on runoff energy which in turn is a function of rainfall and antecedent soil moisture conditions. The runoff energy represents the energy required in detaching and transporting the sediment. Runoff volume and peak runoff rate used for the sediment yield simulation are obtained from the hydrological model [37].

$$\mathrm{SY} = 11.8(Q_{\mathrm{surf}} q_{\mathrm{peak}} A_{\mathrm{hru}})^{0.56} \times K_{\mathrm{USLE}} \times C_{\mathrm{USLE}} \times P_{\mathrm{USLE}} \times \mathrm{LS_{USLE}} \times \mathrm{CFRG} \quad (2)$$

where SY is the sediment yield on a given day (metric tons), Q_{surf} is the surface runoff volume (mm day^{-1}), q_{peak} is the peak runoff rate (m^3 s^{-1}), A_{hru} is the area of the HRU (ha), K_{USLE} is the USLE soil erodibility factor, C_{USLE} is the USLE crop management factor, P_{USLE} is the USLE support practice factor, $\mathrm{LS_{USLE}}$ is the USLE topographic factor, and CFRG is the coarse fragment factor. Sediment routing in the channel is controlled by both the degradation and deposition processes [11]. If the upland sediment load is greater than the transport capacity of the channel, deposition occurs; otherwise, degradation is the most dominant process in the channel.

2.3 SWAT + Model Setup

The modelling process followed a systematic approach. Initially, the default SWAT + model was setup utilizing the data listed in Table 1, which had been pre-processed into SWAT + input data formats. Subsequently, the model was simulated for the period from 1981 to 2020, corresponding to the range of climate input data used. The catchment was delineated into 20 subbasins consisting of 213 LSUs further discretized into 5829 HRUs. Consequently, multi-site hydrological calibration and validation were conducted at the Lake basin outlet and at Gumera river inlet, at a monthly timestep using a period of 1992–2002. Then, the river sediment load was calibrated using reported annual average values. Finally, the temporal and seasonal simulations of sediment load were validated by comparing them to remote sensing (RS) lake turbidity data at the river inlets.

Of specific interest is the RS lake turbidity product. The RS lake turbidity product for Lake Tana was downloaded from the Copernicus Global Land Service (CGLS) at 300-m resolution for the periods 2016–2020. The CGLS for lake water provides remote sensing observations collected within the optical and thermal spectrums using the Medium Resolution Imaging Spectrometer Multispectral (MERIS) sensor onboard ENVISAT and OLCI sensors on board Sentinel-3. The RS product contains corrected water quality parameters, namely lake water surface temperature, lake surface reflectance (LSR), lake turbidity (TUR) and Trophic State Index (TSI), which have been radiometrically and atmospherically corrected [48]. The LSR is given in all the available wavebands after correction and as a normalized dimensionless quantity from which TUR and TSI can be derived [48]. A turbidity product with a temporal resolution of 10 days and spatial resolution of 300 m (version 1.3.0) was used. The turbidity was extracted as 10-day averages (on the 1st, 11th, and 21st day of the month) and resampled to monthly averages.

Table 1 Input data used for the SWAT + model setup

Data type	Resolution	Source
Digital elevation model (DEM)	30 m	Shutter Radar Topography Mission (SRTM; [39])
Land use	300 m for 2015	European Space Agency (ESA; [40])
Soil	250 m	Africa Soil Information Service (AFSIS; [41])
Precipitation	0.05° at daily timestep	Climate Hazards Group InfraRed Precipitation with Station data (CHIRPS; [42])
Temperature, solar radiation, wind speed, and relative humidity	0.5° at daily timestep	GSWP3-W5E5 [43–46]
Observed discharge	Monthly timestep for Gumera River and lake outlet	Bahir Dar University
Reported sediment load	Annual average	[3, 6, 47]
Lake turbidity	300 m at monthly timestep	Copernicus Global Land Service (CGLS; https://land.copernicus.eu/global/products/lwq)

Turbidity serves to indicate underwater light availability as measured relative to water clarity. Total suspended solids (TSS) can strongly influence the water transparency, and hence, TSS estimates in relation to LSR are used to derive TUR. The retrieved parameters for sampled sites are assessed against in situ measurements from various data sources including LIMNADES. LIMNADES is an initiative to establish a database of lake bio-optical measurements that can be used as match up data for remote sensing. Therefore, the information accessed in LIMNADES meets the requirements of being data that represents the surface characteristics of water bodies and thus is reliable and can be used for direct comparison with remote sensing data [49, 50]. It serves as the primary database of optical property datasets and in situ water quality measurements for validating satellite products. The validation also analyzes the consistency of the time series by taking the same 10-day averages for different years during the wet and dry periods [48].

2.4 Model Calibration (Hydrological and Sediment Load)

The sensitivity of the model was carried out using the SWAT + Toolbox, an open-source software for calibrating SWAT + models. The Sobol algorithm was used to conduct a global sensitivity analysis. The model was hydrologically calibrated and validated on a monthly timestep using a multisite approach using flow data available for Gummera River and the lake outlet (Abay), for the period 1991–2002. Model performance was evaluated using the Nash–Sutcliffe (NSE) and the percent bias (PBIAS) [51].

Due to lack of a time series of observed sediment loads, the simulated sediment loading was calibrated based on reported mean annual sediment load values (1994–2016) from previous studies. The calibration was carried out by adjusting the bedload coefficient for individual rivers. The bedload coefficient determines the fraction of incoming sediments in a river that settles as bedload.

2.5 Evaluation of Simulated Temporal Patterns of Sediment Loading with RS

Calibrating the model for mean annual sediment loads does not imply accurate representation of seasonal and long-term temporal patterns of sediment loading. Thus, the seasonal and temporal representation of sediment loads by the model was assessed using the RS Lake turbidity dataset. The turbidity data was extracted as a time series from CGLS at the four river inlets into Lake Tana (Fig. 1). The spatial representativeness of the turbidity values and hence the confidence in the turbidity values was ensured by averaging the values of neighboring pixels around the river inlets to reduce the possibility of selecting outliers. For each river inlet, the extracted turbidity dataset was used to evaluate the simulated river sediment loading from the calibrated SWAT + model. This was done on the premise that the lake turbidity dataset has been globally validated. The seasonality of the SWAT + river sediment load simulations was statistically and graphically assessed for consistency with the RS dataset to assess the performance of the model in representing the seasonal and temporal patterns of sediment loading into the lake from the four rivers.

3 Results

3.1 Flow Simulation

Based on the performance criteria by Moriasi et al. [51], the model calibration results demonstrated excellent performance at a monthly time step in simulating flow for the Gumera River, with NSE values of 0.89 and 0.78 during the calibration and validation phases, respectively (Fig. 2a). The simulations effectively captured the seasonal variations in flow; however, they slightly underestimated the low flows, as indicated by a PBIAS of 1.5% and 4.9% in the calibration and validation periods, respectively (Fig. 2a). At the outlet of the lake (Abay), the model performance was lower but still satisfactory in reproducing the observed flow patterns. The NSE values for the calibration and validation periods were 0.58 and 0.49, respectively (Fig. 2b). The lower model performance at the outlet was also evident from the higher PBIAS, which amounted to 15.9% and 17.8% in the calibration and validation periods, respectively. This lower performance can mainly be attributed to the manual control of outflow from the lake using gates at the outlet leading to the Blue Nile [52]. This manual control makes it challenging to accurately replicate the management operations in the absence of actual data. Nevertheless, the flow performance at the lake outlet does not significantly impact the sediment simulations within the basin under study. Instead, its primary influence is on sediment loadings downstream from this basin, which falls outside the scope of this study.

3.2 Sediment Loading

Sediment loading from the four rivers exhibited a similar temporal pattern to that of river discharge into the lake. The loading increased significantly during the rainy season, peaking over July to August, which coincided with the peak in river flow (Fig. 3). During the dry season, sediment loading is considerably lower due to much lower runoff. Over the period 2016–2020, sediment loads from Gilgel Abay and Gummera Rivers were the highest of the four rivers, with peaks of up to 6 Mt/month (Gilgel Abay) and 3 Mt/month (Gummera) at the peak of the wet season. Ribb and Megech

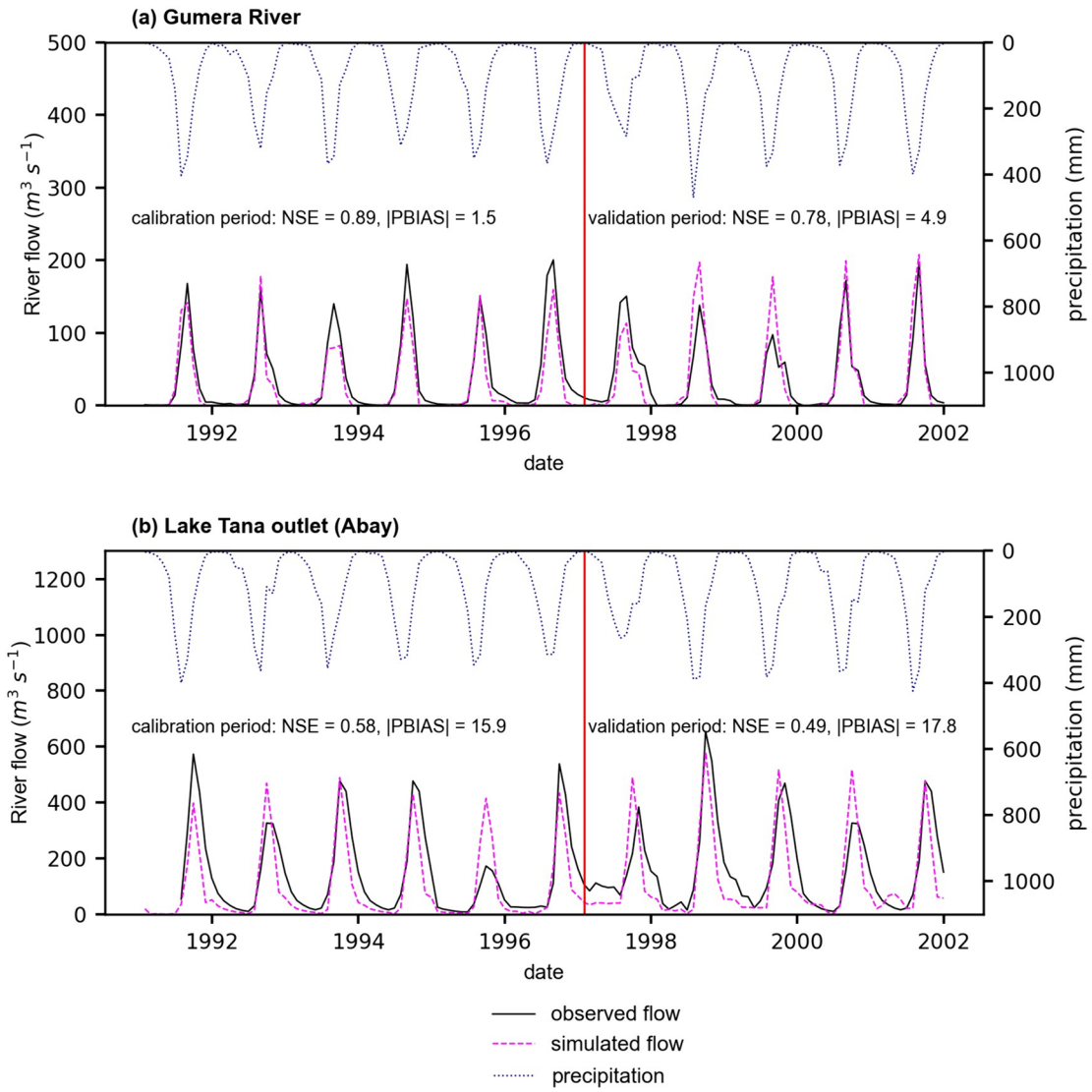

Fig. 2 Model performance at the Gummera River and the Lake Tana outlet (Abay) at monthly timestep

Rivers on the other hand contributed much lower sediment loads peaking about 1 Mt/month during the wet season (Fig. 3). The selected time period of 2016–2020 aligns with the availability of RS lake turbidity data, which is used for validation in the subsequent section.

The calibrated annual average sediment loads for the four rivers were found to be consistent with the reported values of annual averages of river sediment loads from previous studies (Table 2). Collectively, these rivers contribute an estimated 25.2 Mt/yr, with Gilgel Abay and Gummera accounting for over 80% of the total sediment loading into the lake. In these river basins, sediment yield varies between 50 and more than 80 tons/ha/yr and studies have demonstrated that slope gradient, particularly in the hilly headwaters of the sub-catchments, strongly influences sediment yield [6]. Thus, the high sediment loading in these rivers can be attributed to a combination of factors, including significant soil erosion, higher rainfall, soil type, and extensive cropland areas in the respective sub-catchments [6].

As reported by Lemma et al. [47], the trend of sediment yield in the Lake Tana basin follows a general decrease from the south to the west in an anticlockwise direction, which is consistent with the findings of this study. This pattern aligns closely with the distribution of rainfall across the catchment and the relative size of the sub-catchments. The spatial variation in sediment yield and transport into the lake is readily apparent through the extent and intensity of turbidity plumes observed surrounding the lake, as illustrated in Fig. 4. Notably, the areas exhibiting the highest turbidity levels (Fig. 4) correspond to the inflow rivers characterized by the highest sediment loading (Fig. 3), providing a clear indication of the relationship between sediment loading and turbidity.

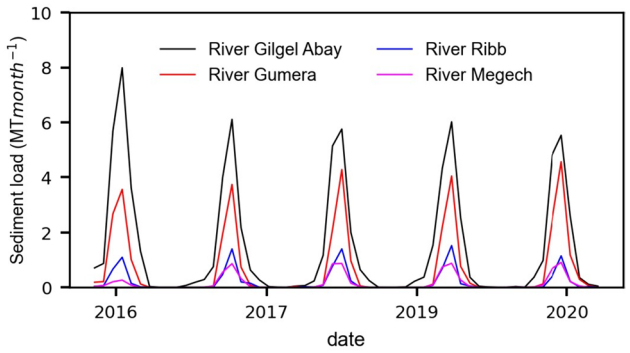

Fig. 3 Simulated monthly SWAT + sediment loading into Lake Tana for selected major rivers

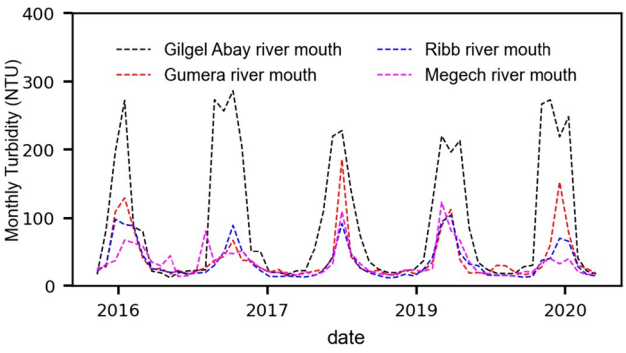

Fig. 4 Time series of monthly RS lake turbidity at the four river inlets into Lake Tana

3.3 Lake Turbidity Hotspot vs River Sediment Load Input

During the dry season (December–May), the monthly remote sensing (RS) turbidity measurements over the lake consistently showed uniformly low turbidity levels, as depicted in Fig. 4. However, at the locations where the four major rivers flow into the lake, turbidity gradually increased from the beginning of the wet season and reached its peak in July to August, before gradually decreasing as the dry season approached (Fig. 5) which shows that the variation of turbidity over the lake is associated with the seasonal variation of regional climate which can carry along sediments and nutrients that end up impacting the turbidity levels of the lake. A similar finding was reported by Moges et al. [24].

The RS turbidity time series data extracted at the river inlets for the four major rivers, along with the spatial distribution of turbidity across the lake, provided compelling evidence that the fluctuation of turbidity in the lake followed the same seasonal pattern as the sediment loading from the four rivers (Fig. 4). Notably, the average annual turbidity recorded at the river inlet of Gilgel Abay was 91.2 NTU, compared to Gummera (41.8 NTU), Ribb (37.8 NTU), and Megech (37.6 NTU) river inlets. The spatial visualization of turbidity across the lake (Fig. 5) demonstrated that, at the peak of the wet season, turbidity at the entry point of the Gilgel Abay River was significantly higher compared to the other river inlets.

Table 2 Average annual simulated sediment loads at river inlets into Lake Tana

River inlet	River sediment load (Mt/yr)		Time period	Source
	Simulated	Observed/reported		
Gilgel Abay	13.24	7.9–14.3	1994–2016	[3, 6, 47]
Gummera	7.70	7.5–8.2		
Ribb	2.54	2.7–3.9		
Megech	1.72	0.9–2.2		

The consistency between the simulated sediment loads for the four rivers and the observed turbidity levels further supported the relationship between high sediment contribution and elevated turbidity around the lake. This relationship also indicated that RS turbidity can be used to identify sediment loading hotspots into the lake. In this study, the entry of Gilgel Abay River emerged as a major sediment hotspot for Lake Tana (Fig. 5). This finding is consistent with a previous study by Kebedew et al. [53], which reported the formation of a peninsula stretching 10 km long and 2 km wide as a result of near shore sediment deposition by River Gilgel Abay. However, it is important to recognize that turbidity is influenced not only by the quantity of sediment loadings but also by the concentrations of nutrients transported within those sediments [54]. Therefore, future studies may benefit from exploring beyond the correlation between turbidity and sediment loadings and consider the relationship between turbidity and the concentration of nutrients carried by sediments.

3.4 Evaluating Seasonality of SWAT + Sediment Loading

The simulated sediment loads from the four tributary rivers were compared to the RS lake turbidity at the river inlets to assess the temporal representation of sediment loads. During the period of 2016–2020, a strong correlation ($R^2 > 0.66$) was observed between the simulated sediment loading and RS lake turbidity for Gilgel Abay, Gummera, and Ribb rivers (Fig. 6). However, the correlation was considerably lower ($R^2 = 0.40$) for River Megech, primarily due to the quality of turbidity data extracted at the river inlet of Megech into Lake Tana. As depicted in Fig. 4, the seasonality of turbidity for River Megech was not adequately captured compared to the other three rivers. This disparity might arise from the considerably smaller river flow, rendering it more susceptible to influences from the lake's prevailing conditions. Alternatively, the presence of wetland areas around River Megech inlet [55] could

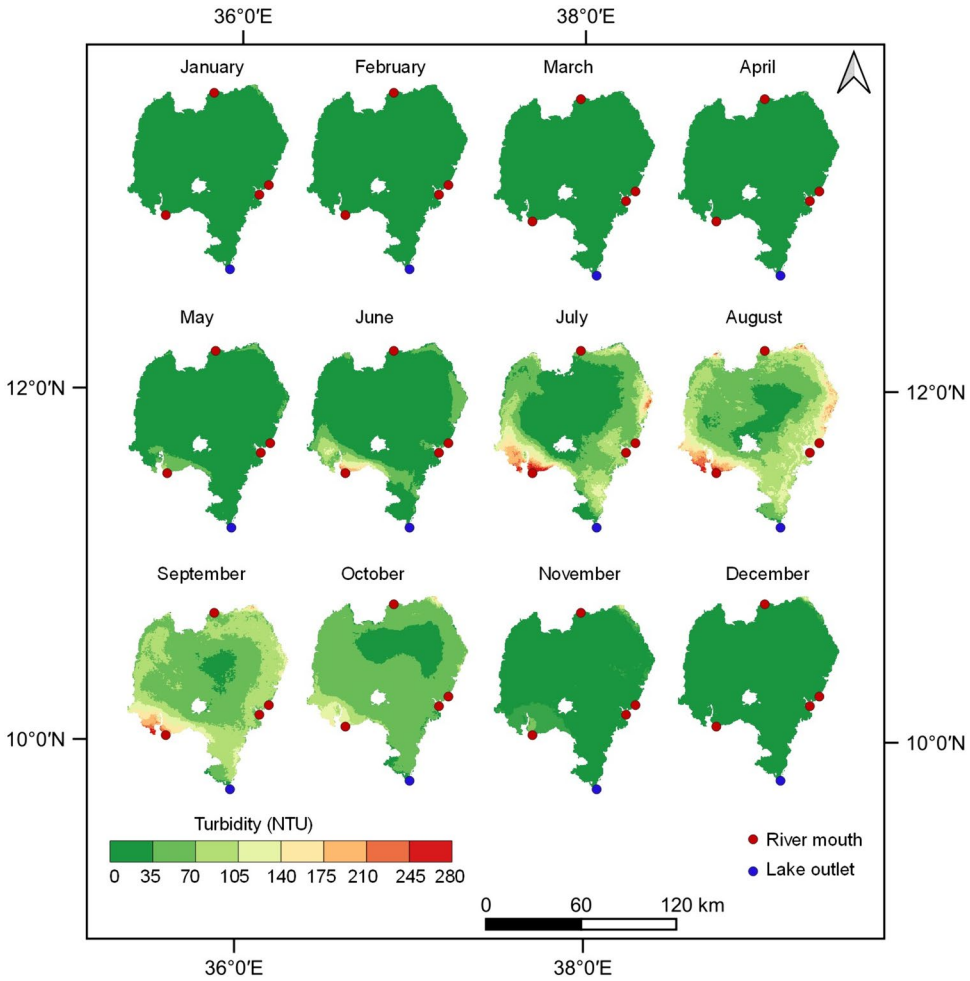

Fig. 5 Long-term mean monthly spatial variation of RS turbidity over Lake Tana from 2016 to 2020

potentially act as a buffer, modifying the river's inflow dynamics into the lake. Notably, the RS turbidity for River Megech only exhibited significant peaks during the wet seasons of 2018 and 2019.

The high correlation observed for the other rivers suggested a strong connection between sediment load and turbidity, indicating that the influx of sediment is a major contributor to lake turbidity. In the case of Gummera and Gilgel Abay rivers, which have substantial sediment loads, the plots demonstrated a stronger correlation for higher values of both turbidity and sediment loading (Fig. 6). This finding highlights the robustness of the simulated sediment loads for these two rivers.

4 Discussion

The strong correlation observed between model-simulated river sediments and RS lake turbidity ($R^2 > 0.66$) at most river inlets provides evidence that the turbidity in the lake is primarily caused by suspended sediment. This finding aligns with the conclusions reached by Womber et al. [56], who also identified relatively higher turbidity concentrations at the inlets of the major tributary rivers during the rainy season. These findings highlight the significant influence of river inflows containing high concentrations of sediments originating from degraded and saturated runoff areas within the lake basins, which is consistent with the findings of our study.

Of specific focus in this study was the correlation of the model-simulated river sediments and RS lake turbidity. The results demonstrated that even though the SWAT + model was solely calibrated for mean annual sediment loading values, it adequately captured the seasonality and temporal variations of sediment loading for the four rivers considered in this study. Except for the Megech River inlet, the simulated sediment loading exhibited a strong correlation ($R^2 > 0.66$) with remote sensing turbidity. The robustness of the RS turbidity dataset was also evident in its ability to represent the seasonal and spatial patterns of turbidity across the lake, enabling the identification of hotspots for incoming sediment loading. These findings highlight the potential of RS water quality products as a valuable option for evaluating water quality models, particularly in regions with limited data availability. Our findings align with previous studies

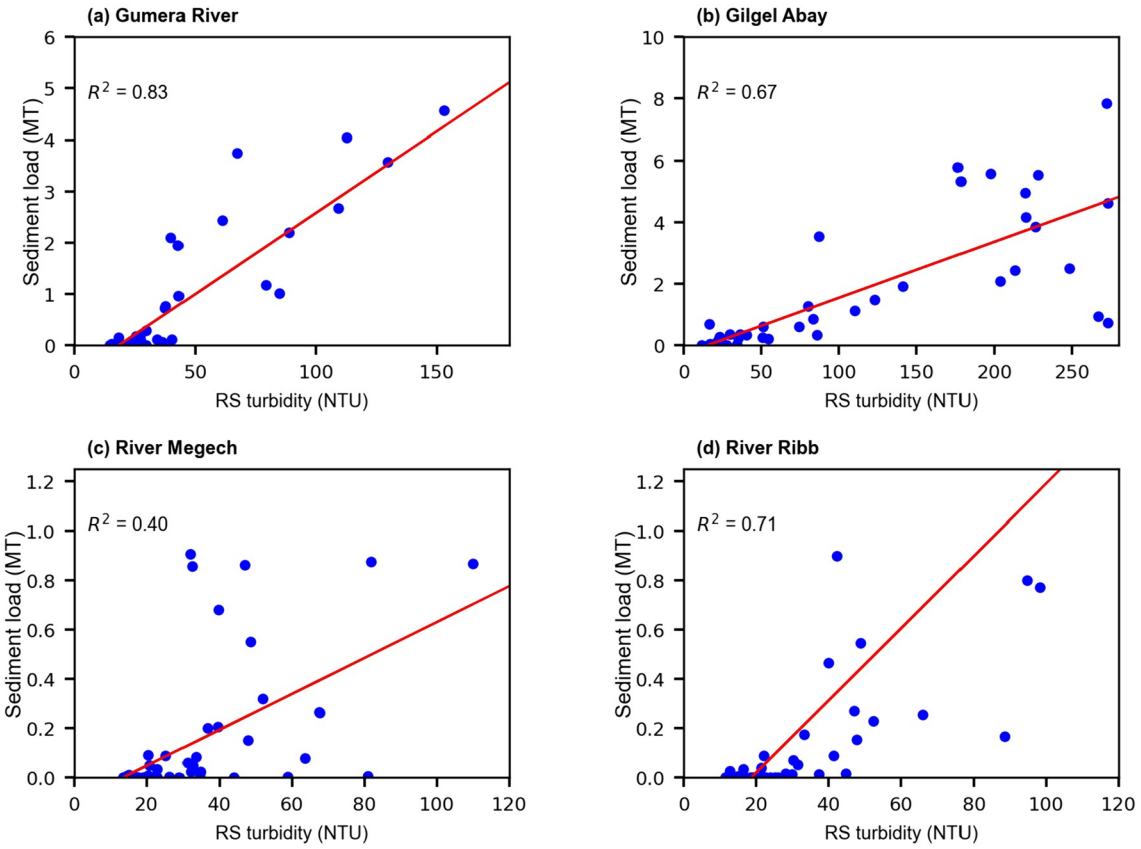

Fig. 6 Correlation of monthly RS turbidity and SWAT + sediment loading at river inlets of the four major rivers

in the basin [25, 57], which utilized regression equations to derive historical suspended sediment concentrations and turbidity from RS MODIS-Terra images for the Gumera River inlet. The results indicated a linear relationship between sediment concentrations and RS turbidity, with $R^2 > 0.76$. However, the authors acknowledged various sources of uncertainty associated with employing regression statistics to derive data from RS products, and they also highlighted the lack of transferability of regression equations from one river to another.

While assessing the performance of the model, it is also important to recognize the limitations of RS lake turbidity product used in this study. One major challenge is that the turbidity product is derived from an optical sensor which is susceptible to atmospheric conditions such as interference by clouds. This affects lake surface reflectance and the retrieval of turbidity especially during the wet season when cloud cover can be significant. As already seen for the case of Megech River, the inconsistency in seasonal turbidity may have occurred due to the interference by clouds. The possibility of using a multi-sensor monitoring approach could be explored in the future, in order to overcome this limitation. Another limitation arises from the averaging of lake turbidity over days where atmospheric conditions are not homogeneous. This can lead to maps available in patches of data over the lake and data that is inconsistent. Additionally, even though global validation has been carried out for the turbidity product, there has been no known validation campaign that has been conducted for Lake Tana, an indication of some level of uncertainty associated with the quality of the RS product. In addition, atmospheric correction of reflectance data may introduce systematic errors that may affect the quality of turbidity pixels in the remote sensing product. Finally, the comparative analysis of both the remote sensing and SWAT + sediment loading in this study was conducted over only 5 years (2016–2020) as remote sensing turbidity from Sentinel 3 was not available prior to this period. Thus, the general findings arrived at from this study should be interpreted with caution given the short period of overlap between the two datasets.

5 Conclusions

The increasing rate of land use change, land degradation, and soil erosion in the Tana basin poses a critical threat to the water resources, fishery, and agricultural productivity of the region. Monitoring sediment loading into the receiving water bodies is thus important not only to safeguard water quality and

productivity of these water bodies but also to monitor the rate of land degradation and devise mitigatory management strategies to reduce soil erosion and guarantee the sustainability of land-based resources. However, the applicability of physical models to model sediment trends and support decision making in the basin has been restricted by the scarcity of in situ sediment data which is required to evaluate these models. This study bridges the gap by utilizing RS lake turbidity data to conduct a comprehensive comparison with simulated model sediment loads from four rivers within the Lake Tana basin.

Results from the SWAT + model indicated that Gilgel Abay and Gummera rivers contributed the highest sediment loading into the lake with annual average values of 13.24 Mt/yr and 7.7 Mt/yr respectively, jointly contributing more than 80% of sediment loading into the lake. River Ribb contributed 2.54 Mt/yr while River Megech which drains the smallest of the four sub catchments contributed only at 1.72 Mt/yr. A comparison between simulated sediment load from the four inflow rivers and RS lake turbidity at the river inlet locations revealed that the simulated sediment loading and turbidity exhibit a similar seasonal pattern as evidenced by a high correlation coefficient. Additionally, locations of the highest turbidity corresponded with those where river sediment loading was highest enabling the identification of sediment loading hotspots in the lake using the turbidity data. Thus, RS lake turbidity data potentially provides a valuable alternative source of data to assess simulated temporal and spatial variability of river sediment loading in the absence of in situ data. However, the effects of local specific conditions, such as water hyacinth coverage, geological conditions, and existing infrastructures in the basins, are worth considering when estimating turbidity with respect to sediment concentration. Additionally, unless constrained by data availability, evaluating model performance with in situ measurements is always advisable.

These findings provide planners and decision makers with an additional support tool to devise catchment management measures that can address the land degradation problems in the basin and the deteriorating quality of water in the lake. It is also important to note that the turbidity levels of Lake Tana, as observed through remote sensing, are relatively high and have shown an upward trend over time. Hence, continuous monitoring is of vital importance for effective lake management and comprehensive assessment.

Acknowledgements The authors thank the Research Foundation – Flanders (FWO) for funding the International Coordination Action (ICA) "Open Water Network: Open Data and Software tools for water resources management" (project code G0E2621N), the Open Water Network: impacts of global change on water quality (project code G0ADS24N), the AXA Research Chair fund on Water Quality and Global change and the King Baudouin Foundation for the Ernest du Bois Prize Fund (agreement No. 2022-F2812650-228938).

Author Contribution Conceptualization: A.N and R.E.G. Methodology, analysis, and writing: R.E.G, A.N, K.L, E.A.Y. Result interpretation: All authors. Review: A.v.G, A.B.M, T.T.

Funding This work was supported by the Research Foundation – Flanders (FWO) for funding the International Coordination Action (ICA) "Open Water Network: Open Data and Software tools for water resources management" (project code G0E2621N), the Open Water Network: impacts of global change on water quality (project code G0ADS24N), the AXA Research Chair fund on Water Quality and Global change and the King Baudouin Foundation for the Ernest du Bois Prize Fund (agreement No. 2022-F2812650-228938).

Data Availability The SWAT + model is publicly available at https://swat.tamu.edu/software/plus/, the remote sensing turbidity data is available at https://land.copernicus.eu/global/products/lwq, the soil map [41] is downloadable from https://www.isric.org/projects/africa-soil-information-service-afsis, the digital elevation model [39] is downloadable from https://cgiarcsi.community/data/srtm-90m-digital-elevation-database-v4-1/, observed weather data of minimum and maximum temperature, solar radiation, humidity, and wind speed [42–45] is downloadable from https://doi.org/https://doi.org/10.5880/pik.2016.004, the CHIRPS precipitation data [42] can be downloaded from https://www.chc.ucsb.edu/data/chirps, and the land use map from ESA [40] can be downloaded from https://www.esa-landcover-cci.org/?q=node/164. Analysis and processing of data was done using Python and R scripts. Scripts can be obtained from the corresponding author upon request.

Declarations

Ethical Approval Not applicable.

Competing Interests The authors declare no competing interests.

References

1. Nkwasa, A., Chawanda, C. J., & van Griensven, A. (2022). Regionalization of the SWAT+ model for projecting climate change impacts on sediment yield: An application in the Nile basin. *Journal of Hydrology Regional Studies, 42*, 101152. https://doi.org/10.1016/j.ejrh.2022.101152
2. Lemma, H., Frankl, A., van Griensven, A., Poesen, J., Adgo, E., & Nyssen, J. (2019). Identifying erosion hotspots in Lake Tana Basin from a multisite Soil And Water Assessment Tool validation: Opportunity for land managers. *Land Degradation and Development, 30*(12), 1449–1467. https://doi.org/10.1002/ldr.3332

3. Zimale, F. A., et al. (2018). Budgeting suspended sediment fluxes in tropical monsoonal watersheds with limited data: The Lake Tana basin. *Journal of Hydrology and Hydromechanics, 66*(1), 65.
4. Abebe, W. B., & Minale, A. S. (2017). *Land use and watershed management practices in Lake Tana*. In: Basin social and ecological system dynamics. Springer, Cham, pp 479–521.
5. Bogale, A. (2020). Review, impact of land use/cover change on soil erosion in the Lake Tana Basin, Upper Blue Nile, Ethiopia. *Applied Water Science, 10*(12), 235. https://doi.org/10.1007/s13201-020-01325-w
6. Lemma, H., et al. (2018). Revisiting lake sediment budgets: How the calculation of lake lifetime is strongly data and method dependent. *Earth Surface Processes and Landforms, 43*(3), 593–607. https://doi.org/10.1002/esp.4256
7. Setegn, S. G., Srinivasan, R., Dargahi, B., & Melesse, A. M. (2009). Spatial delineation of soil erosion vulnerability in the Lake Tana Basin, Ethiopia. *Hydrological Processes: An International Journal, 23*(26), 3738–3750.
8. Vijverberg, J., Sibbing, F. A., & Dejen, E. (2009). *Lake Tana: Source of the Blue Nile*. In: Dumont HJ (ed) The Nile. Monographiae Biologicae, vol 89. Springer, Dordrecht. https://doi.org/10.1007/978-1-4020-9726-3_9
9. Teshale, B., Lee, R., & Zawdie, G. (2002). Development initiatives and challenges for sustainable resource management and livelihood in the Lake Tana region of Northern Ethiopia. *International Journal of Technology Management and Sustainable Development, 1*(2), 111–124.
10. Wondie, A., et al. (2012). Preliminary assessment of water hyacinth (*Eichornia crassipes*) in Lake Tana, in: Proceedings of the National Workshop (Biological Society of Ethiopia), Addis Ababa, Ethiopia.
11. Arnold, J. G., Srinivasan, R., Muttiah, R. S., & Williams, J. R. (1998). Large area hydrologic modeling and assessment part i: Model development1. *JAWRA Journal of the American Water Resources Association, 34*(1), 73–89. https://doi.org/10.1111/j.1752-1688.1998.tb05961.x
12. Bieger, K., et al. (2017). Introduction to SWAT+, a completely restructured version of the Soil And Water Assessment Tool. *JAWRA Journal of the American Water Resources Association, 53*(1), 115–130. https://doi.org/10.1111/1752-1688.12482
13. Chakilu, G. G., Sándor, S., Zoltán, T., & Phinzi, K. (2022). Climate change and the response of streamflow of watersheds under the high emission scenario in Lake Tana sub-basin, upper Blue Nile basin, Ethiopia. *Journal of Hydrology: Regional Studies, 42*, 101175.
14. Setegn, S. G., Rayner, D., Melesse, A. M., Dargahi, B., & Srinivasan, R. (2011). Impact of climate change on the hydroclimatology of Lake Tana Basin, Ethiopia. *Water Resources Research, 47*, 1–13. https://doi.org/10.1029/2010WR009248
15. Tenaw, M., & Awulachew, S. B. (2009). *Soil and water assessment tool (SWAT)-based runoff and sediment yield modeling: a case of the Gumera watershed in Lake Tana sub basin.* Intermediate Results Dissemination Workshop held at the International Livestock Research Institute (ILRI), Addis Ababa, and Ethiopia. pp 100–111
16. UNEP, A. (2016). *A snapshot of the world's water quality: towards a global assessment.* Nairobi: United Nations Environment Programme (UNEP) 162 pp.
17. Yasir, S. A., Crosato, A., Mohamed, Y. A., Abdalla, S. H., & Wright, N. G. (2014). Sediment balances in the Blue Nile River basin. *International Journal of Sediment Research, 29*(3), 316–328.
18. Dörnhöfer, K., & Oppelt, N. (2016). Remote sensing for lake research and monitoring – Recent advances. *Ecological Indicators, 64*, 105–122. https://doi.org/10.1016/j.ecolind.2015.12.009
19. Dube, T., Mutanga, O., Seutloali, K., Adelabu, S., & Shoko, C. (2015). Water quality monitoring in sub-Saharan African lakes: A review of remote sensing applications. *African Journal of Aquatic Science, 40*(1), 1–7. https://doi.org/10.2989/16085914.2015.1014994
20. Ritchie, J. C., Zimba, P. V., & Everitt, J. H. (2003). Remote sensing techniques to assess water quality. *Photogrammetric Engineering and Remote Sensing, 69*(6), 695–704. https://doi.org/10.14358/PERS.69.6.695
21. Yunus, A. P., Masago, Y., & Hijioka, Y. (2020). COVID-19 and surface water quality: Improved lake water quality during the lockdown. *Science of the Total Environment, 731*, 139012. https://doi.org/10.1016/j.scitotenv.2020.139012
22. Vanhellemont, Q., & Ruddick, K. (2021). Atmospheric correction of Sentinel-3/OLCI data for mapping of suspended particulate matter and chlorophyll-a concentration in Belgian turbid coastal waters. *Remote Sensing of Environment, 256*, 112284. https://doi.org/10.1016/j.rse.2021.112284
23. Papa, F., et al. (2023). Water resources in Africa under global change: Monitoring surface waters from space. *Surveys In Geophysics, 44*(1), 43–93. https://doi.org/10.1007/s10712-022-09700-9
24. Moges, M. A., Schmitter, P., Tilahun, S. A., Ayana, E. K., Ketema, A. A., Nigussie, T. E., & Steenhuis, T. S. (2017). Water quality assessment by measuring and using Landsat 7 ETM + images for the current and previous trend perspective: lake. *Journal of Water Resources Protection, 9*, 1564–1585. https://doi.org/10.4236/jwarp.2017.912099
25. Kaba, E., Philpot, W., & Steenhuis, T. (2014). Evaluating suitability of MODIS-Terra images for reproducing historic sediment concentrations in water bodies: Lake Tana, Ethiopia. *International Journal of Applied Earth Observation and Geoinformation, 26*, 286–297.
26. Taffese, T., Tilahun, S. A., & Steenhuis, T. S. (2014). Phosphorus modeling, in Lake Tana Basin, Ethiopia. *Journal of Environment and Human, 2*, 47–55.
27. Setegn, S. G., Srinivasan, R., & Dargahi, V. (2008). Hydrological modelling in the Lake Tana Basin, Ethiopiausing SWAT model. Hydrological modelling in the Lake Tana basin, Ethiopia, using SWAT model. *The Open Hydrology Journal, 2*, 49–62.
28. Lemma, H., Nyssen, J., Frankl, A., Poesen, J., Adgo, E., & Billi, P. (2019). Bedload transport measurements in the Gilgel Abay River, Lake Tana Basin, Ethiopia. *Journal of Hydrology, 577*, 123968. https://doi.org/10.1016/j.jhydrol.2019.123968
29. Demissie, S., et al. (2022). Effects of soil bund spacing on runoff, soil loss, and soil water content in the Lake Tana Basin of Ethiopia. *Agricultural Water Management, 274*, 107926. https://doi.org/10.1016/j.agwat.2022.107926
30. Getachew, B., & Manjunatha, B. R. (2022). Impacts of land-use change on the hydrology of Lake Tana Basin, Upper Blue Nile River Basin, Ethiopia. *Global Challenges, 6*(8), 2200041. https://doi.org/10.1002/gch2.202200041
31. Dile, Y. T., Berndtsson, R., & Setegn, S. G. (2013). Hydrological response to climate change for Gilgel Abay River, in the Lake Tana Basin - Upper Blue Nile Basin of Ethiopia. *PLoS ONE, 8*(10), e79296. https://doi.org/10.1371/journal.pone.0079296
32. Wubie, M. A., Assen, M., & Nicolau, M. D. (2016). Patterns, causes and consequences of land use/cover dynamics in the Gumara watershed of lake Tana basin, Northwestern Ethiopia. *Environmental Systems Research, 5*(1), 8. https://doi.org/10.1186/s40068-016-0058-1
33. Moges, M. A., Schmitter, P., Tilahun, S. A., & Steenhuis, T. S. (2018). Watershed modeling for reducing future non-point source sediment and phosphorus load in the Lake Tana Basin, Ethiopia. *Journal of Soils and Sediments, 18*(1), 309–322. https://doi.org/10.1007/s11368-017-1824-z
34. Goshu, G., & Aynalem, S. (2017). Problem overview of the Lake Tana Basin, in Social and ecological system dynamics: Characteristics, trends, and integration in the Lake Tana Basin, Ethiopia. In K. Stave, G. Goshu, & S. Aynalem (Eds.), *AESS Interdisciplinary*

Environmental Studies and Sciences Series (pp. 9–23). Cham: Springer International Publishing. https://doi.org/10.1007/978-3-319-45755-0_2
35. Nkwasa, A., Chawanda, C. J., Msigwa, A., Komakech, H. C., Verbeiren, B., & van Griensven, A. (2020). How Can We Represent Seasonal Land Use Dynamics in SWAT and SWAT + Models for African Cultivated Catchments? *Water, 12*, 1541. https://doi.org/10.3390/w12061541
36. Nkwasa, A., Waha, K., & van Griensven, A. (2022). Can the cropping systems of the Nile basin be adapted to climate change? *Regional Environmental Change, 23*(1), 9. https://doi.org/10.1007/s10113-022-02008-9
37. Neitsch, S. L., Arnold, J. G., Kiniry, J. R., & Williams, J. R. (2011). Soil and Water Assessment Tool TheoreticalDocumentation, Version 2009. Temple, Tex.: Texas Water Resources Institute Technical Report No. 406.
38. Nkwasa, A., Chawanda, C. J., Jägermeyr, J., & van Griensven, A. (2022). Improved representation of agricultural land use and crop management for large-scale hydrological impact simulation in Africa using SWAT+. *Hydrology and Earth System Sciences, 26*(1), 71–89. https://doi.org/10.5194/hess-26-71-2022
39. Farr, T. G., Rosen, P. A., Caro, E., Crippen, R., Duren, R., Hensley, S., Kobrick, M., Paller, M., Rodriguez, E., Roth, L., Seal, D., Shaffer, S., Shimada, J., Umland, J., Werner, M., Oskin, M., Burbank, D., & Alsdorf, D. (2007). The shuttle radar topography mission. *Reviews of Geophysics, 45*(2). https://doi.org/10.1029/2005RG000183
40. Defourny, P., et al. (2012). Land cover CCI. *Product User Guide Version, 2*(325), 10–1016.
41. Hengl, T., et al. (2015). Mapping soil properties of Africa at 250 m resolution: Random forests significantly improve current predictions. *PLoS ONE, 10*(6), e0125814.
42. Funk, C., Peterson, P., Landsfeld, M., Pedreros, D., Verdin, J., Shukla, S., Husak, G., Rowland, J., Harrison, L., Hoell, A. & Michaelsen, J. (2015) The climate hazards infrared precipitation with stations—A new environmental record for monitoring extremes. *Scientific Data, 2*, 150066. https://doi.org/10.1038/sdata.2015.66
43. Dirmeyer, P. A., Gao, X., Zhao, M., Guo, Z., Oki, T., & Hanasaki, N. (2006). GSWP-2: Multimodel analysis and implications for our perception of the land surface. *Bulletin of the American Meteorological Society, 87*(10), 1381–1398.
44. Kim, H., Watanabe, S., Chang, E. C., Yoshimura, K., Hirabayashi, J., Famiglietti, J., & Oki, T. (2017). Global Soil Wetness Project Phase 3 Atmospheric Boundary Conditions (Experiment 1). *Data Integration and Analysis System (DIAS)*. https://doi.org/10.20783/DIAS.501
45. Lange, S. (2019). *EartH2Observe, WFDEI and ERA-Interim data Merged and Bias-corrected for ISIMIP (EWEMBI).* V.1.1. GFZ Data Services. https://doi.org/10.5880/pik.2019.004
46. Cucchi, M., et al. (2020). WFDE5: Bias-adjusted ERA5 reanalysis data for impact studies. *Earth System Science Data, 12*(3), 2097–2120.
47. Lemma, H., Frankl, A., Dessie, M., Poesen, J., Adgo, E., & Nyssen, J. (2020). Consolidated sediment budget of Lake Tana, Ethiopia (2012–2016). *Geomorphology, 371*, 107434. https://doi.org/10.1016/j.geomorph.2020.107434
48. Stelzer, K., Simis, S. Muller, D., and Selmes, N. (2020). Copernicus global land operations 'cryosphere and water' quality assessment report - Lake water quality 300m and 1km products. https://land.copernicus.eu/global/sites/cgls.vito.be/files/products/CGLOPS2_ATBD_LWQ300_1km_v1.3.1_I1.12.pdf
49. Tyler, A. N., Hunter, P. D., Spyrakos, E., Neil, C., Simis, S., Groom, S., Merchant, C. J., Miller, C. A., O'Donnell, R., & Scott, E. M. (2017) A global observatory of lake water quality EGU General Assembly Conf. Abstracts p 10609.
50. Groom, S., Tyler, A., Hunter, P., Spyrakos, E., Martinez-Vicente, V., Merchant, C., Cutler, M., Rowan, J., Dawson, T., Maberly, S., Cavalho, L., Elliot, A., Thackery, S., Miller, C., & Scott, M. (2014). GloboLakes: a global observatory of lake responses to environmental change. – In: EGU general assembly conference abstracts. EGU General Assembly Conference Abstracts, p. 14124.
51. Moriasi, D. N., Gitau, M. W., Pai, N., & Daggupati, P. (2015). Hydrologic and water quality models: Performance measures and evaluation criteria. *Transactions of the ASABE, 58*(6), 1763–1785.
52. Dessie, M., et al. (2015). Water balance of a lake with floodplain buffering: Lake Tana, Blue Nile Basin, Ethiopia. *Journal of Hydrology, 522*, 174–186. https://doi.org/10.1016/j.jhydrol.2014.12.049
53. Kebedew, M. G., Tilahun, S. A., Zimale, F. A., & Steenhuis, T. S. (2020). Bottom sediment characteristics of atropical lake: Lake Tana, Ethiopia. *Hydrology, 7*(1), 18. https://doi.org/10.3390/hydrology7010018
54. Worqlul, A. W., Ayana, E. K., Dile, Y. T., Moges, M. A., Dersseh, M. G., Tegegne, G., & Kibret, S. (2020). Spatiotemporal dynamics and environmental controlling factors of the Lake Tana water hyacinth in Ethiopia. *Remote Sensing, 12*(17). https://doi.org/10.3390/rs12172706
55. Wondie, A. (2018). Ecological conditions and ecosystem services of wetlands in the Lake Tana Area, Ethiopia. *Ecohydrology and Hydrobiology, 18*(2), 231–244. https://doi.org/10.1016/j.ecohyd.2018.02.002
56. Womber, Z. R., et al. (2021). Estimation of suspended sediment concentration from remote sensing and in situ measurement over Lake Tana, Ethiopia. *Advances in Civil Engineering, 2021*, e9948780. https://doi.org/10.1155/2021/9948780
57. Ayana, E. K., Worqlul, A. W., & Steenhuis, T. S. (2015). Evaluation of stream water quality data generated from MODIS images in modeling total suspended solid emission to a freshwater lake. *Science of the Total Environment, 523*, 170–177. https://doi.org/10.1016/j.scitotenv.2015.03.132